Low-Cost Instrument for Whispering Gallery Mode Thermometry up to 19 GHz

Low-cost Instrument for Whispering-Gallery Thermometry up to 19 GHz

Simone Corbellini, Chiara Ramella, Marco Pirola, Vito Fernicola, Andrea Cappella

***Abstract*—In this paper we present the architecture and validation of a portable low-cost system for the accurate measurement of complex resonance frequencies up to 19 GHz for whispering gallery thermometry. In this framework the proposed instrument can become the key element to enable the use of whispering gallery thermometers as transfer standards in industrial field. The proposed instrument performs vector S_{21} measurements with ppb-level accuracy in the determination of resonance frequency. Thanks to a compact removable frequency extension module, the system covers two different RF/microwave bands: 800 MHz to 7 GHz and 13 GHz to 19 GHz. The low-frequency band is suitable for quasi-spherical-resonator-based experiments, currently of great interest in different metrological applications, while the high-frequency band has been expressly conceived for whispering gallery thermometry applications. The instrument has been validated using an extremely stable set-up based on quasi-spherical resonator. Calibration of the low-cost whispering gallery thermometer composed of an existent resonator and the proposes system has been performed. The results obtained prove the suitability of the measurement system to replace vector network analyzers in accurate resonance-based experiments and the potential accuracy of the low-cost whispering gallery thermometer.**

***Index Terms*—microwave resonance measurement, whispering gallery thermometry**

I. Introduction

A key element for a widespread dissemination of thermodynamic temperature within the industrial world, is the availability of simple, robust and low-cost thermometers and transfer standards. Industrial application field, covering the temperature range between -196 °C to +500 °C, is currently dominated by Platinum Resistance Thermometers (PRTs), providing uncertainties from nearly 10 mK down to 1 mK (Standard PRTs). However, an alternative solution is strongly desirable, capable to overcome the mechanical sensitivity issue that affects PRTs, making them extremely difficult and expensive to handle and transfer [1]. A very promising candidate to replace PRTs, is represented by the Whispering Gallery Mode Thermometer (WGMT), which is far less sensitive to mechanical shocks and can potentially provide lower uncertainties. In 2007 a sapphire-based WGMT, was first proposed by NIST [2], showing uncertainty better than 10 mK from -40 °C to 85 °C and repeatability at ice melting point better than 1 mK. More recently, INRiM also developed different prototypes [3,4], achieving sub-millikelvin resolution and repeatability, and demonstrating a sensor interchangeability at level of ± 40 mK [5], thus confirming the results found by NIST and further encouraging the investigation of WGMTs.

A WGMT consists of a sapphire resonator (axially symmetric mono-crystalline sapphire), whose resonance frequency is related to temperature by the relation [6]

$$\frac{1}{f_0}\frac{\partial f_0}{\partial T} \approx \frac{1}{f}\left(\frac{\partial f_0}{\partial \varepsilon_\perp}\frac{\partial \varepsilon_\perp}{\partial T} + \frac{\partial f_0}{\partial \varepsilon_\parallel}\frac{\partial \varepsilon_\parallel}{\partial T}\right) \tag{1}$$

where $\varepsilon_\perp$ and $\varepsilon_\parallel$ are the dielectric permittivities in the radial and axial direction, respectively. Such resonator is suspended in a metallic resonant cavity, which has the twofold function of coupling the EM field to the resonator and, above all, to preserve the surface of the sapphire from impurities and humidity. This is crucial to keep the high quality factor (Q) typical of whispering gallery mode resonances, between 20,000 and 90,000 [2,4]. Even if the manufacturing cost of a WGMT is comparable or even lower than that of a PRT, these high Qs pose demanding requirements on the employed measurement set-up that must rely on high-performance Vector Network Analyzers (VNA). However such VNAs can be extremely expensive, even more than accurate PRT thermometry bridges.

Moreover, accurate VNAs are usually bulky instruments, and thus represent a major limit to the application of WGMTs as transfer standards. Hence the need for a portable and low-cost system for the accurate measurement of microwave resonance frequencies. Such a system can also bring advantages in many other metrological applications, since resonance-based innovative primary or transfer standards have been presented for pressure [7] and humidity [8], while concerning temperature it can also apply to acoustic thermometry [9,10]. Since in all these applications the frequency range of interest is known *a priori*, a high-accuracy system affording limited functionalities with respect to a VNA can be built at a fraction of its cost and with reduced volume, thus enabling field portability.

In this paper, we present the development of a VNA-like accurate, low-cost, portable instrument covering frequencies up to 19 GHz, a range that is tailored to Whispering Gallery Thermometry application [2]–[5]. After briefly discussing the WGMT characteristics and requirements in Section II, we detail the system's architecture and features in Section III. In Section IV the experimental validation of the system is presented, while in Section V the calibration of the WGMT system composed of the developed set-up and an existent whispering gallery mode thermometer from INRiM is discussed. Finally some conclusions are drawn in Section VI.

S. Corbellini, M. Pirola and C. Ramella are with the Department of Electronics and Telecommunications, Politecnico di Torino, Corso Duca degli Abruzzi, 24 - 10129, Torino (Italy); e–mail: simone.corbellini@polito.it

V. Fernicola is with the Thermodynamics Division, Istituto Nazionale di Ricerca Metrologica, Strada delle Cacce, 91 - 10135, Torino (Italy)

A. Cappella is with the Laboratoire Commun de Métrologie, LNE-CNAM (LCM), Rue du Landy, 61 - 93210 La Plaine St Denis (France)

II. WGMT MEASUREMENT REQUIREMENTS

The developed instrument requirements have been tailored to the characterization of the spherical-sapphire-based WGMT developed by INRiM and presented in [4]. The resonator, shown in Fig. 1, is a 12 mm-diameter mono-crystalline sapphire sphere suspended inside a 24 mm-diameter, 24 mm-height cylindrical copper cavity. The cavity comprises a cylinder body, and two disks to seal it at top and bottom. Vacuum sealing is obtained with two o-rings between body and disks. The cavity is gold-plated in order to increase surface electrical conductivity and thus improve electrical contact between the body and the disks. From INRiM characterization campaign [5], the more suitable resonance modes for thermometry applications turned out to be WGM3 around 13.6 GHz, WGM4 around 16.4 GHz and WGM5 around 19 GHz. Among these, WGM3 is the strongest one and has been used in the characterization reported in [5] and for the preliminary tests reported in [11].

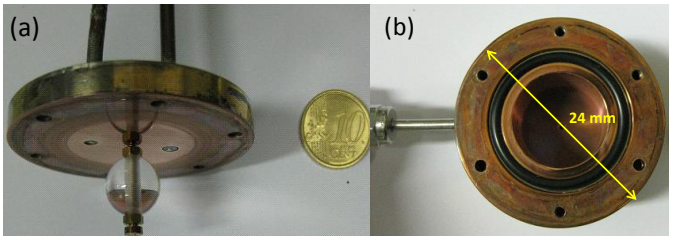

Fig. 1. Picture of the spherical-sapphire-based WGMT from INRiM.

A resonance measurement, usually consists in measuring the transmission parameter S_{21} of the resonator. In fact, even if in principle also the reflection parameter S_{11} could be exploited, the almost unitary background reflection makes it more difficult to accurately detect weak peaks in this case. The system requirements posed by the WGMT application are summarized in Table I. Vectorial S_{21} measurements are necessary in order to compensate for systematic errors, and typical frequency values, for resonators with tens of millimeter diameter, are between 13 GHz and 19 GHz [2]–[5]. From the amplitude stand-point, considering a typical peak amplitude of 10 dB to 40 dB above transmission background and the possible variability of transmission levels in different experiments, a minimum dynamic range of 70 dB is required.

The target temperature measurement uncertainty is of few millikelvins: considering that the average sensitivity of the WGMT prototypes by NIST and INRiM is around -60 ppb/mK [2]–[5], the resonance frequency must be known with an accuracy of few parts per billion (ppb) to ensure a negligible contribution to the thermometer uncertainty. Concerning the reference frequency, it has to be at least stable at ppb-level not to limit the potential resolution of the WGMT.

III. MEASUREMENT SYSTEM ARCHITECTURE

The measuring instrument we propose is outlined in Fig. 2. It is composed of four functional block: 1) the instrument's core, which is a stand-alone 800 MHz to 7 GHz vector S_{21}-meter proposed by the authors in [12,13] for the characterization of energy gases, application that also relies on detection of resonances in RF cavities, 2) a frequency extension module to cover the target 13 GHz to 19 GHz bandwidth for WGMT applications, 3) a frequency division module to generate a reference signal at 10 MHz and 4) the frequency reference module designed as a low cost alternative to frequency standard references to achieve the desired ppb-level accuracy (see Table I).

Operating frequency range	13 GHz - 19 GHz
Dynamic range	$\geq$ 70 dB
Resonant frequency measurement uncertainty (after fitting)	$\leq$ 10 ppb
Frequency reference accuracy	$<$ 10 ppb
Frequency reference stability	1 ppb
Other system requirements	Low cost Compactness Low power consumption

TABLE I
SYSTEM REQUIREMENTS FOR WGMT APPLICATION.

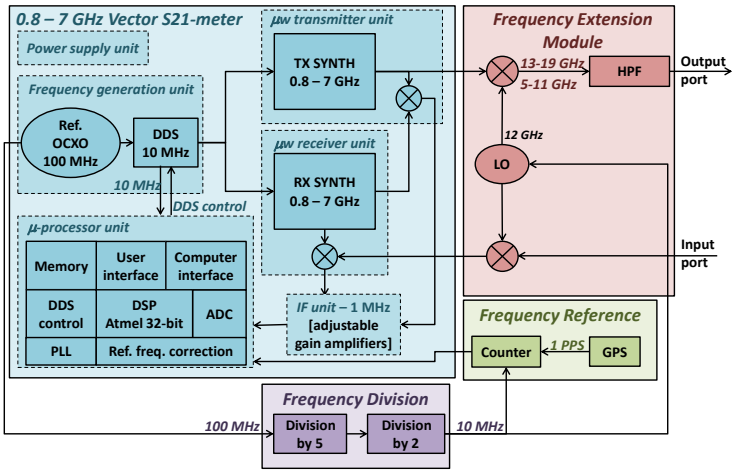

Fig. 2. Block diagram of the proposed instrument.

A. Double bandwidth vector S_{21}-meter

In order to keep the instrument architecture as simple as possible, single-step frequency conversion from RF/microwave to ADC frequency is preferable. While this can be easily achieved at RF, also with cheap components, it becomes increasingly difficult moving toward higher frequencies. Given the need of a two-step-conversion system, the most convenient choice was to re-use the 800 MHz - 7 GHz instrument already available together with add-on modules *ad-hoc* designed to address the new features required by the WGMT application. This solution allows to maintain the overall architecture very simple and thus to use low-cost components. Finally, modularity of the measuring system provides great flexibility yielding to a unique compact instrument able to cover two different bandwidths. The extension of the instrument also to the intermediate 7 GHz to 13 GHz bandwidth, currently not covered, can be easily achieved with a further module.

The core S_{21}-meter (0.8 GHz - 7 GHz) comprises several functional blocks as highlighted in Fig. 2. The processing unit, in charge of providing user and computer interface and the necessary computing capability to perform control and signal processing functions, is the *Atmel* AT32UC3C0512C 32-bit microprocessor equipped with 16 12-bit, 2 MSa/s analog-to-digital converters (ADC) and 512 KB memory. The RF/microwave section of the instrument comprises the transmitter and the receiver: two distinct sets of synthesizers are employed for transmission and demodulation. Each set counts three low-cost variable synthesizers by *Synergy Microwave Corporation* (LFSW80120-100, LFSW190410-100, LFSW397697-100), each covering approximately an octave and having 1 MHz frequency step. According to the measurement bandwidth selected by the user, the microprocessor automatically enables the appropriate synthesizer. Since the low resolution of these cheap synthesizers is unable to match the instrument requirements, a direct-digital-synthesizer (DDS) is used to provide all the instrument elements with a finely tuned clock, thanks to which 10 ppb resolution for the generated signal is achieved. Note that the special DDS-generated clock is applied to all the instrument functional blocks, including the microprocessor, in order to maintain coherency and improve the measurement signal-to-noise ratio (SNR). This solution allows for coherent sub-sampling at the ADC level, thus enabling the use of a simplified 3-parameter sine-fit algorithm [14,15] for signal processing. The adopted DDS is the AD9954 from *Analog Devices*, and it is driven by a 100 MHz oven-controlled crystal oscillator (OCXO) from *Abracon Corporation* (model AOCJY3A) with ± 1 ppb/day aging. The receiver unit performs single-step down-conversion to 1 MHz, which is an intermediate frequency (IF) suitable for direct analog-to-digital conversion. Wide-range programmable-gain amplifiers (PGA) (*Analog Devices* AD8369) are used to increase the overall dynamic range up to more than 100 dB. A detailed outline of the microwave front-end is reported in Fig. 3 (left): all the employed high-frequency components are low-cost off-the-shelf devices by *Mini Circuits*.

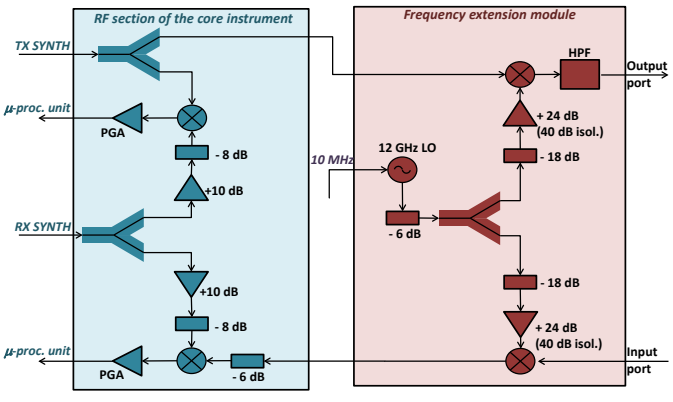

Fig. 3. Detailed block diagram of RF/microwave parts of the core instrument and frequency extension module.

The frequency extension module (Fig. 2 and Fig. 3-right) performs a single step frequency conversion from the original 0.8 GHz - 7 GHz bandwidth to the target 13 GHz (12.8 GHz) - 19 GHz range, employing a 12 GHz local oscillator (LO): the SPC-ESP-12000-06 form *EM Research*. Since a high-frequency oscillator is an expensive components (approximately 2000 $), only one LO has been used from both up- and down-conversion in conjunction with a high pass filter (HPF) to suppress the low-band product frequencies and avoid superposition after down-conversion. The selected filter is the EW437 from *BSC Filters* that has 12 GHz to 20 GHz low-ripple band-pass. The filter, that costs approximately 1000 $ represents the second main contribution to the overall system cost, but it can be omitted if the cavity under test has no resonances in the image frequency range. All the other parts are cheap components from *Mini Circuits*.

B. Frequency reference module

The measurement uncertainty of the double bandwidth S_{21}-meter described so far is mainly determined by the reference frequency: the internal OCXO was targeted to the energy gas characterization set-up [12,13], which was based on ratiometric measurements and thus posing stringent requirements only on short-term stability. To fit the WGMT requirements (see Table I) a ppb-level accurate and stable frequency reference is mandatory. The option of locking the core instrument to an external reference instead of the OCXO was foreseen during the design phase, adding a dedicated input port. To achieve the desired accuracy and stability, a high quality frequency standard would be required, which is however too expensive and bulky to match the goal of this work. To overcome this issue we therefore propose an alternative low-cost frequency reference, implemented by adding an extremely compact module (see Fig. 2) to the set-up and a couple of specialized functions to the digital processor.

The frequency reference module is inspired to the Global Positioning System Disciplined Oscillator (GPSDO) approach [16], whose main advantages are the very low cost (below 100 $) and the fact that it requires no calibration. With the GPSDO technique, the clock accuracy and stability are guaranteed by the atomic oscillators through the 1 pulse-per-second (1PPS) timing signal available in almost any off-the-shelf GPS receiver. In classical GPSDO architectures, the 1PPS signal, synchronized to the Coordinated Universal Time (UTC) with just few nanosecond jitter, is used to lock a local oscillator. In our system, instead, it is used to accurately measure, by means of a dedicated counter, the local clock. The main advantage of this solution is that, it introduces no clock perturbations since it avoids direct feedback to the OCXO. The OCXO signal is divided by 10 to obtain a 10 MHz signal and then measured using the 1PPS signal from the GPS (*Tyco* A1029-A-01 GPS receiver) as gating for the counter (*Atmel* ATmega-328 microcontroller) over a 100 s sliding observation window. The result of the count is received by the core instrument processor which provides a feedback to the DDS to adjust its 10 MHz output before starting a measure (note that the DDS does not allow ppb-level adjustment) and corrects the residual frequency error of each measured resonance.

C. Frequency division module

This dedicated module, enclosed in an aluminium shield to improve EM isolation and noise performances, is in charge of dividing by 10 the 100 MHz signal form the OCXO. 10 MHz frequency reference is the standard value for laboratory equipment, thus its availability enables the use of the proposed system to lock other instruments in complex experiments. The 10 MHz signal is also needed by the frequency extension module to drive the 12 GHz local oscillator. The frequency reference module counts this 10 MHz signal, instead of directly measuring the 100 MHz output. In this way the minimum necessary observation window is larger, but the requirements on the counter are more relaxed, allowing for the use of a simpler microprocessor and avoiding further circuit complexity. The 100 s observation interval required by this solution is not a concern since the selected OCXO is stable enough over this window [11]. Division by 10 is performed with two ICS87001 programmable clock dividers from *Integrated Device Technology*. The first perform a division by 5, while the second a division by 2, thus ensuring the 50% output duty cycle, required for proper working of the LO.

The complete measurement system implemented is shown in Fig. 4, the prototype cost is around 5000 $, which is more than one order of magnitude lower than a VNA with comparable accuracy.

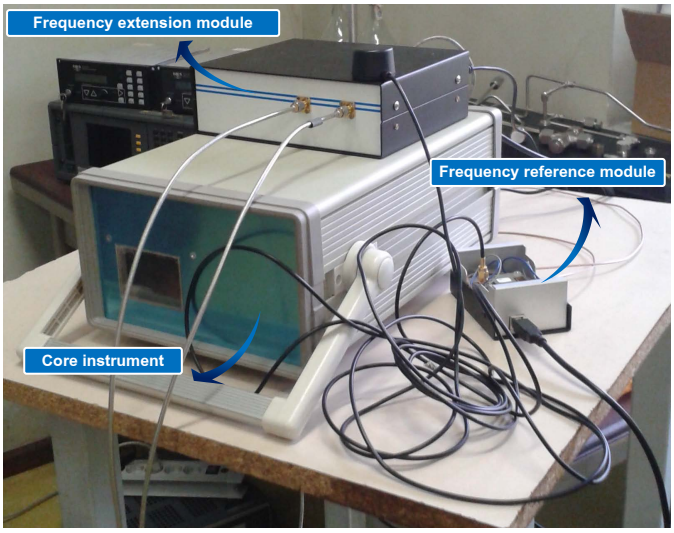

Fig. 4. Picture of the proposed measurement set-up.

D. Resonance fitting algorithm

The spectrum gathered from S_{21} measurements must be fitted with a proper function in order to find the complex resonance frequency $f_0 = f + jg$, where f is the frequency of the peak and g the half-power bandwidth. Therefore a dedicated fitting algorithm has been implemented in Matlab-like environment. The theoretical model for a resonance is the Lorentzian function [2]. However, in order to account also for the unavoidable transmission background we added a quartic polynomial. Finally, in order to make the algorithm suitable also for degenerated resonances (doublet and triplet) we added two more optional Lorentzian functions:

$$S_{21} = \frac{\alpha_0 f}{f^2 - f_0^2} + \sum_{n=0}^{4} \beta_n (f - f_c)^n + \left(\sum_{m=1}^{2} \frac{\alpha_m f}{f^2 - f_m^2} \right) \quad (2)$$

where f_c is the center frequency of the measurement frequency range, while α_0 (α_1, α_2), β_n and f_0 (f_1, f_2) are the complex parameters to be fitted. The fitting algorithm employed is based on the Lavenberg-Marquardt method which minimizes the least-squared residuals of both real and imaginary parts [19] of Eqn. 2. The software plots the real time trend of the resonance frequency (or the mean of the resonance frequencies) during a measurement session, giving a quick feedback to the user on the stability of the experiment.

IV. Experimental validation of the system

Achieving high performance from a measuring system composed by low-cost parts and conceived to keep the architecture as simple as possible is a challenging goal. Therefore a thorough experimental characterization has to be performed to validate the instrument. Moreover, when a system with a high level of expected accuracy has to be tested, also arranging the test bench to assess it is not trivial. In fact, the intrinsic accuracy limits of the bench itself can come out to be the dominant contribution to measurement uncertainty, thus making it impossible to appreciate the potential performance of the instrument under test. A preliminary assessment of the proposed instrument has been reported by the authors in [11], where we compared the instrument accuracy with that achievable with a high-performance VNA. However, the set-up in [11], despite being suitable to verify the proper functioning of the system and to compare it to a commercial VNA, proved to be inadequate to demonstrate the best achievable instrument performance. In particular, the results found in [11], also reported in Fig. 5, show three critical aspects:

1) *poor temperature stability*: during observation a significative temperature drift (around 25 ppb/h) was encountered, thus we had to use least-square fitting to be able to compare the measurements from the two instruments
2) *poor accuracy*: measurement standard deviation was about 17 ppb, a value which is higher than the expected achievable accuracy. Since this value was approximately the same both for the VNA measurements and those gathered with the proposed instrument, we can ascribe this poor accuracy to the set-up
3) *offset between absolute values*: an unexpected 100 ppb offset between the absolute frequency values obtained with the two instruments was recorded. This aspect was object of further investigation whose results are discussed below (Section IV-A)

In order to overcome the issues encountered in [11], a final experimental validation has been performed, employing a ppb-level-stable experimental set-up from LNA-CNAM [17,18] equipped with a state-of-the-art VNA for comparison.

The present Section is organized following the chronological order of the performed experiments: first we discuss the offset issue and its solution, then we present the experimental

results obtained with the LNE-CNAM set-up, demonstrating the actual instrument accuracy.

A. The offset issue: effect of phase rotation along microwave cables on fitting

In [11] we reported the first results obtained in measuring the WGMT resonance around 13.6 GHz, comparing the results obtained with the developed instrument to those gathered from a commercial VNA. The comparison between the measurement results, reported also in Fig. 5, showed a 100 ppb ($\sim$1.7 mK) discrepancy between the absolute frequencies obtained with the two set-ups. Investigation showed that the responsible for this offset is the fitting algorithm: when the transmission background is high the fitting algorithm hardly copes with the phase rotation over the measurement bandwidth. This phase rotation, that can be clearly seen in Fig. 6 reporting an example of fitting of $\angle S_{21}$, is generated along the microwave cables employed to connect the instrument to the resonator, whose length is not negligible in the bandwidth of interest [11]. In classical VNA-based measurement set-up, the effect of phase rotation is cancel out through calibration at the resonator reference plane. However, in the WGMT case, this approach is practically impossible since the cables are welded to the cavity.

To solve this problem, the phase rotation has been numerically corrected before fitting the transmission spectra. The algorithm employed to automatically find the correct entity of this correction, is based on the minimization of fit residuals. Fig. 7 shows the fit residuals obtained for 4 different spectra as a function of the applied phase correction: all the curves show an absolute minimum around 13.5 °/MHz. Employing 12 spectra, the mean value of the minimum resulted to be (13.4 ± 0.2) °/MHz (1σ). Applying this correction to the measurements of Fig. 5, we obtained the results of Fig. 5(b): the two clouds of measurement points are overlapped and the residual discrepancy between the two fit lines is only 3.3 ppb ($\sim$55 μK). Also the difference between the slope of the two fit lines decreased from the initial 2.52 ppb/h to 0.72 ppb/h. Note that correction has effect also on the VNA measurements, even if in this case the impact is lower. The sensitivity of the absolute resonance frequency to the phase correction resulted, in fact, of 3.8 ppb MHz/° for the designed instrument (overall effect 80 ppb change) and only 0.1 ppb MHz/° (overall effect 18 ppb) for the VNA. These results achieved are very satisfactory, but highlight that special precautions connected to the phase rotation have to be taken when the calibration can not be performed, as is the case of this WGMT.

The developed algorithm for finding the optimum correction coefficient by residual minimization applied on at least 3 measurements, has been embedded within the processing software and applied to all subsequent measurements. The spectrum reported in Fig. 11(b) is an example of corrected spectrum.

B. Validation of the instrument

The LNE-CNAM experimental set-up function is to measure resonances of Quasi-Spherical Resonators (QSR) and was

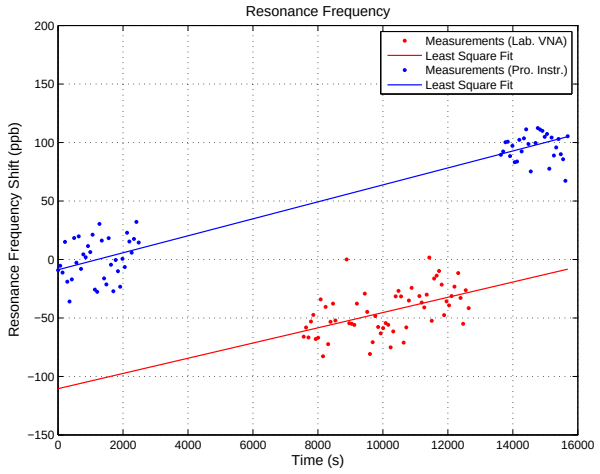

(a) Original measurements.

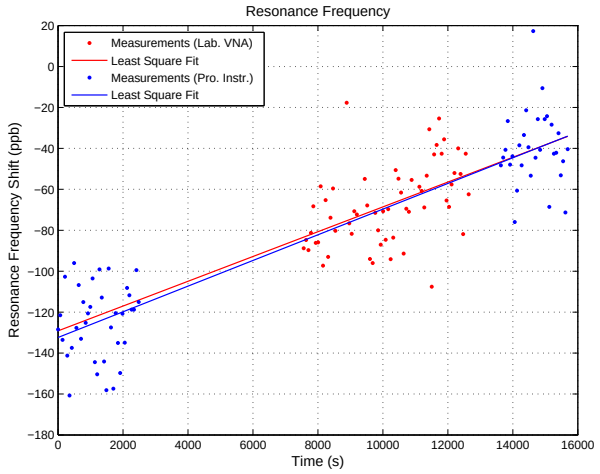

(b) Corrected measurements.

Fig. 5. Comparison between consecutive measurements of resonance frequency: proposed instrument (blue dots) and laboratory VNA (red dots).

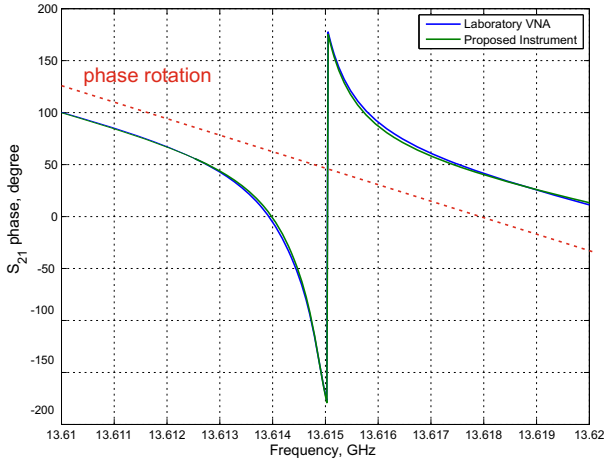

Fig. 6. Example of fitting of $\angle S_{21}$ with highlighted background phase rotation.

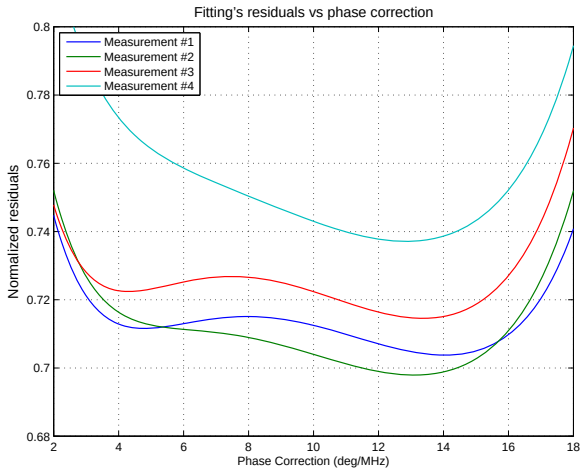

Fig. 7. Example of 4 fit residuals (consecutive measurements) as a function of the applied phase correction.

originally developed for mixed acoustic-microwave temperature measurements [17]. After that, a high-performance temperature stabilization system has been added in order to make the set-up suitable for acoustic-based Boltzmann constant k_B [18] measurements. Within this framework, microwaves are used to accurately determine the shape of the resonator, to improve measurement accuracy. In a QSR, the geometry is deliberately non-spherical so as to lift the degeneracy of modes that would result in any case from unavoidable sphere imperfections. Therefore three different diameters must be measured. Loop antennas are used in order to excite both TE and TM modes, which is important since they have different boundary conditions on the surface of the resonator. For instrument validation a ∼9 cm diameter (90.074 mm, 90.134 mm and 90.194 mm, respectively) has been adopted, focusing on the TE13 mode with resonance around 5.77 GHz. The thermostat employed was designed to resemble a low temperature cryostat: it is composed of a vacuum chamber in which conductive and convective heat transfers are minimized and it is equipped with a thermal shield to reduce radiative heat transfer. The thermostat is immersed in a temperature-controlled liquid bath maintained at a temperature close to that of the triple point of water. Because of the vacuum insulation and the radiation shield, bath oscillations up to several millikelvins do not affect the thermal stability of the acoustic resonator. Four thermometers, two on the radius and two at the poles, are employed, each calibrated to within 0.1 mK, achieving a resolution of 10 μK: no temperature gradients have been encountered within 50 μK and temperature homogeneity of the sphere remains unchanged at the level of 0.1 mK. The novel feature of this set-up is that it isolates the contributions of the various sources of heat (acoustic, microwave, gas flow). This is possible thanks to the quasi-adiabatic cryostat, and it is obtained by electrical substitution. The dominant cause of temperature instability is the room temperature change, which is however compensated by changing the temperature of the heat shield, thus achieving 0.1 mK/day drift only. Since the time constant for thermalization of the 3 dm^3 sphere is 8 hours, the temperature difference between the shell and the gas is less than 32 μK. Argon gas is flowed through the sphere during measurement and its temperature and pressure are monitored and controlled. In this way the measurement error due to changes in the refractive index of Argon as a function of density can be corrected. The impedance of the inlet and outlet tubes created a pressure difference between the upstream and downstream parts of the gas manifold. The upstream pressure is measured with a Digiquartz 745 manometer, while in downstream a rotating piston gauge is employed for servo-control of pressure. Knowing lengths and radii of the tubes the pressure in the QSR can be estimated using the Hagen–Poiseuille equation [18]. In Fig. 8 the measurement results obtained monitoring the QSR temperature and pressure over approximately 6 days are reported, proving the extremely good stability of the set-up, which makes it actually possible to verify the real potential of the developed instrument.

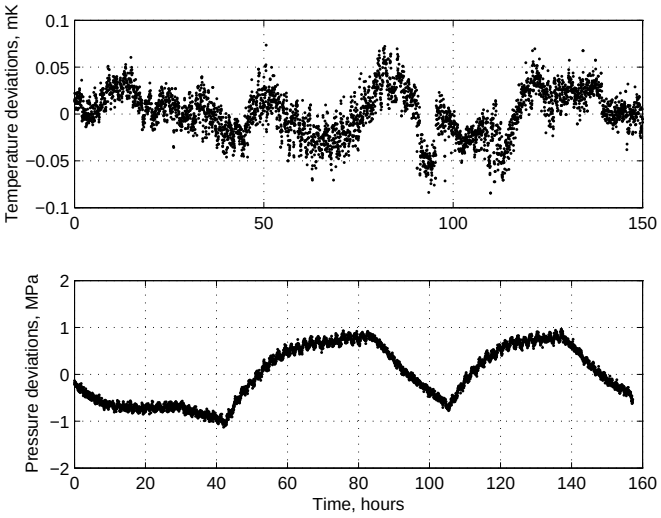

Fig. 8. Temperature and pressure stability of the LNE-CNAM set-up.

The TE13 resonance mode of the QSR has been selected: the resonance triplet is around 5.77 GHz and has been fitted with the sum of 3 Lorentzian functions, as shown in Fig. 9

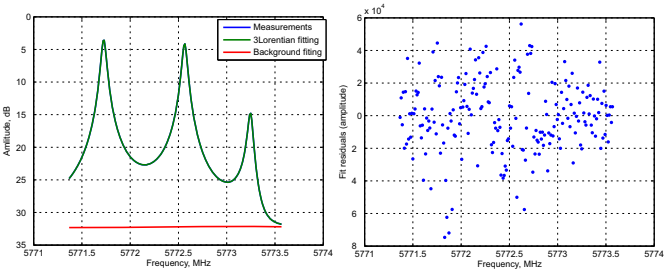

Fig. 9. QSR resonance triplet fitting: resonance amplitude (left) and fit residuals (right).

The QSR has been monitored for 15 hours, gathering one spectrum any 74 s. Each spectrum has been fitted finding three complex resonant peaks, then the average complex frequency

has been computed for each measurement obtaining the results reported in Fig. 10. In this figure the deviations from the mean value of this average frequency are reported, demonstrating that they are within 3 ppb peak-to-peak (1σ=1.2 ppb). From Fig. 10 and Fig. 8 it is clear that these fluctuations are partially due to the set-up. Results are in line with those obtained with the VNA as shown in Table II. The discrepancy between the obtained values is 1.7 ppb, which is comparable with the stability and drift of the employed set-up, thus demonstrating that the proposed instrument can effectively replace VNAs even in experiments requiring high accuracy.

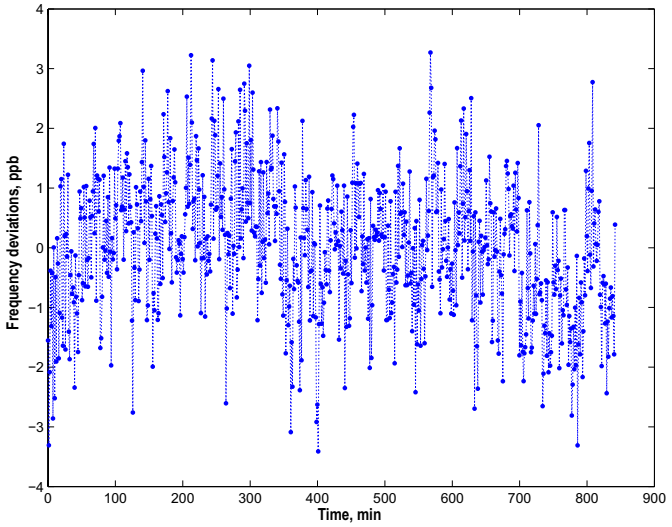

Fig. 10. QSR frequency deviations observed with the proposed instrument over 15-hour monitoring.

	Mean value	1σ
VNA	5772512456.8 Hz	1.4 ppb
Proposed instrument	5772512466.7 Hz	1.2 ppb

TABLE II
QSR RESONANCE FREQUENCY MEASUREMENT RESULT: COMPARISON BETWEEN THE PROPOSED INSTRUMENT AND A COMMERCIAL VNA.

The tests carried out at LNE-CNAM do not use the frequency extension module. However, the accuracy results found at 5.77 GHz apply also to the 13 GHz to 19 GHz range provided that the frequency extension module does not introduce non-linear effects. The fit residuals reported in [11], already suggest the linearity of the system, as they showed no systematics. This is confirmed also by the results in Fig. 11, reporting an example of fitted spectrum and relative residuals.

V. WGMT CALIBRATION

The test bench employed for calibration is shown in Fig. 12: a *Fluke* 7381 precision thermal bath available at INRiM has been adopted which guarantees a minimum 5 mK stability but actually, in many conditions can achieve 1 mK or less stability just with proper setting on the control parameter. For the measurement of temperatures above 0 °C the bath is filled with distilled and de-ionized water. The WGMT immersed

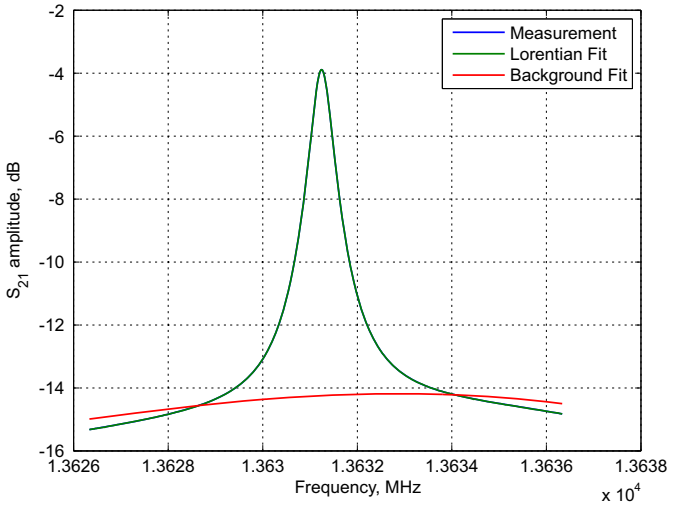

(a) Amplitude.

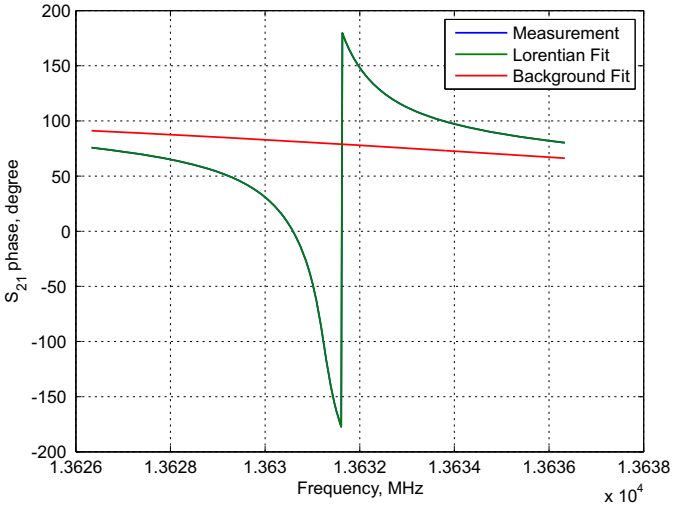

(b) Phase.

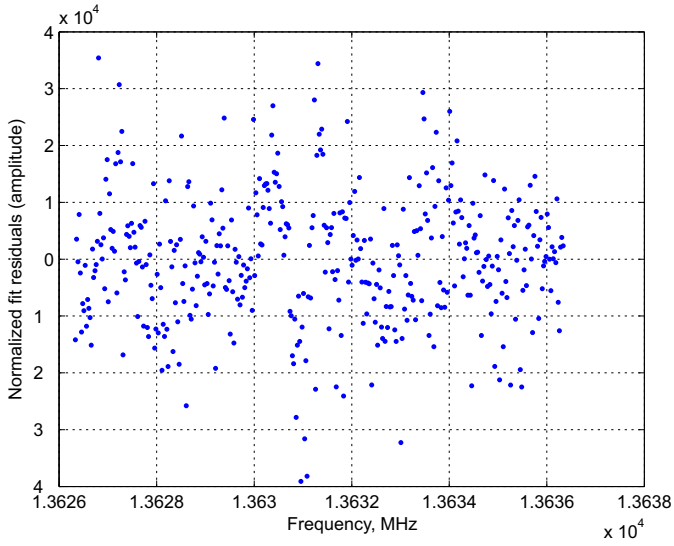

(c) Amplitude fit residuals.

Fig. 11. Example of fitted WGMT resonance spectrum.

in the bath is kept connected to a vacuum pump during the entire test campaign in order to stabilize the cavity maintaining the sapphire surface unperturbed. A Fluke PRT-5620 standard platinum resistance (SPRT), calibrated with 5 mK uncertainty, has been used as reference thermometer in conjunction with the thermometry bridge *Hart Scientific* 1590. A dedicated software was in charge to collect both the WGMT and the SPRT responses and to change the bath temperature every 6 hour approximately. The explored temperature range goes from 10 °C to 85 °C, with 5 °C step.

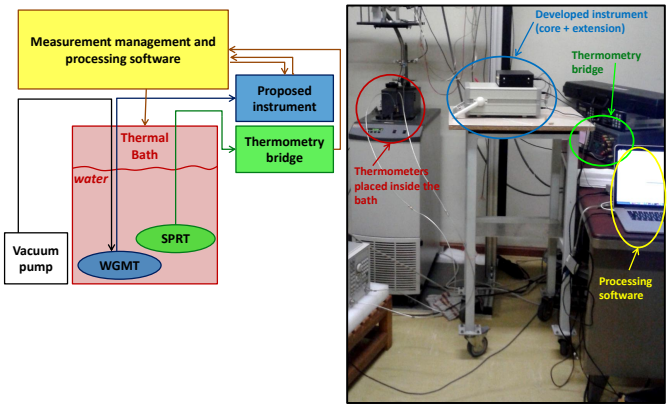

Fig. 12. Picture of the WGMT measurement set-up at INRiM.

Fig. 13 shows an example of measurement response in a 4-hour observation window at the average temperature of around 60 °C. The bath temperature oscillations are within ±0.5 mK, which proves the good stability of the available thermal set-up. The standard deviation of the mean for the WGMT points (∼200 points) is ∼2 ppb, that corresponds to less than 50 μK, confirming the very high resolution achievable by the measuring system.

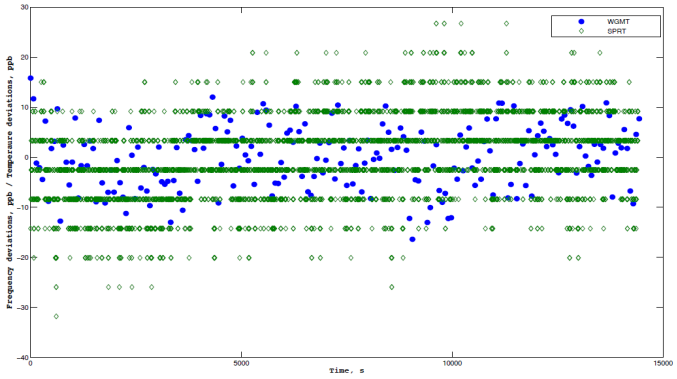

Fig. 13. Comparison of WGMT frequency deviations and SPRT temperature deviations over 4 hours at 60 °C.

A cubic polynomial of the form

$$f_0 = a_0 + a_1 T + a_2 T^2 + a_3 T^3 \qquad (3)$$

has been used as calibration curve model. The subset of temperatures {10, 15, 20, 30, 40, 50, 75, 80, 85} °C has been used to extract the model parameters whose fitted values are reported in Table III. The average sensitivity, obtained from the linear coefficient, is -60 ppb/mK, which is consistent with the result reported in [4,5]. The calibration fit residuals are within ±1 mK, as reported in Fig. 14 (blue points). A second subset of temperatures, namely {25, 35, 45, 60} °C, has been used as test points to verify the calibration curve. As we can see from Fig. 14 (green spots), the deviation of the measurements form the calibration curve are within the range of the fit residuals, thus proving that the cubic polynomial is a suitable function to model the thermometer response in the 10 °C to 85 °C range.

a_0	13615982605 Hz	a_2	-608.29553 Hz/K^2
a_1	-827068.129 Hz/K	a_3	1.36706215 Hz/K^3

TABLE III
CALIBRATION COEFFICIENTS, CUBIC POLYNOMIAL FITTING.

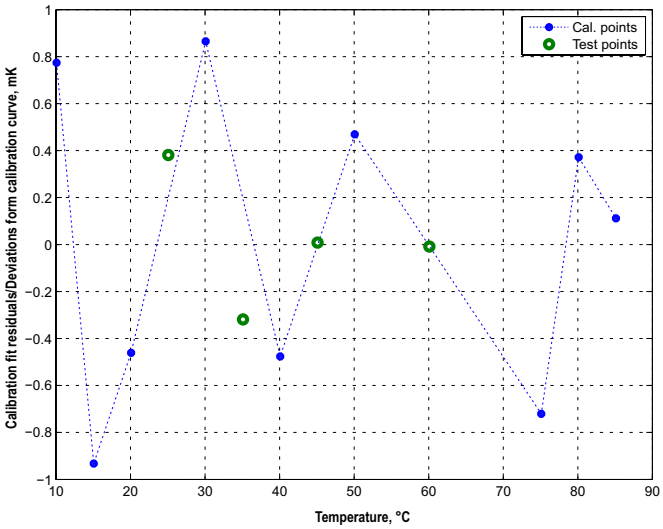

Fig. 14. Calibration fit residuals and measurement deviations from calibration curve.

The main contributions to the uncertainty budget for this experiment are summarized in Table IV: the low accuracy of the available SPRT represents at present the main limit to the measurement uncertainty, while adopting a more accurate SPRT the potential uncertainty of the WGMT system would be in the order of 1 mK.

Frequency reference accuracy	$< 20\,\mu$K
Lorentzian fit repeatability	0.2 mK
Calibration curve fit	1 mK
Short-term repeatability WGMT	0.4 mK
Reference SPRT calibration	5 mK

TABLE IV
UNCERTAINTY BUDGET FOR THE LOW-COST WHISPERING-GALLERY-BASED THERMOMETER.

VI. CONCLUSIONS

A compact, low-cost measurement system for the accurate detection of complex resonance frequencies up to 19 GHz

has been reported and validated. Aim of this set-up is to replace VNA in measuring the response of whispering gallery thermometers, thus enabling their use as transfer standards in industrial applications. Despite being expressly conceived to match WGMT requirements, the proposed system can be of great interest in all those applications where portability and cost-saving are crucial requirements. The implemented prototype price is around 5000 $ and weights about 3 kg. The actual version of the instrument covers two separated frequency ranges: 800 MHz to 7 GHz and 13 GHz to 19 GHz, however thanks to its modularity it would be extremely simple to adapt it to other bandwidths and fully replace VNA in laboratory tests. Moreover, specialized narrow-band modules can be developed, based on the architecture here presented, at even lower cost for application to specific resonators. The system includes an extremely compact low-cost GPS-based frequency reference with ppb-level accuracy and stability, making the instrument autonomous without the need of expensive and bulky frequency standards. A thorough validation, carried out within an extremely stable set-up, is presented, demonstrating the instrument's high-performance. The calibration of a WGMT in the range 10 °C to 85 °C is also reported, achieving ∼5 mK uncertainty, proving its potential effectiveness in replacing PRTs in industrial applications.

This work was supported by EURAMET and the European Union under an EMRP Researcher Grant.

REFERENCES

[1] "NOTED - Novel Techniques for Traceable Temperature Dissemination", EMRP Joint Research Project, Online:http://www.notedproject.com/

[2] G.F. Strouse, "Sapphire whispering gallery thermometer," *Int. J. Thermophys*, vol. 28, pp. 1812–1821, 2007.

[3] L. Yu, V. Fernicola, "A Temperature Sensor Based on a Whispering Gallery Mode Resonator," *Proc. AIP ITS9*, vol. 1552, pp. 920–924, 2012.

[4] L. Yu, V. Fernicola, "Spherical-sapphire-based Whispering Gallery Mode Resonator Thermometer," *Rev. Sci. Instrum.*, vol. 83, pp. 094903-1–5, 2012.

[5] L. Yu, V. Fernicola, "Investigation of Sapphire-based Whispering-gallery Mode Resonators as Tranfer Standard Themometers," *Meas. Sci. Technol.*, vol. 24, pp. 055106-1–5, 2013.

[6] M.E. Tobar *et al*., "Dielectric Frequency-temperature-compensated Microwave Whispering-gallery-mode Resonators," *J. Phys. D: Appl. Phys.*, vol. 30, pp. 2770–2775, 1997.

[7] J.W. Schmidt *et al*., "Polarizability of Helium and Gas Metrology," *Phys. Rev. Lett.*, pp. 245504, 2007.

[8] R. Underwood *et al*., "A microwave resonance dew-point hygrometer," *Meas. Sci. Technol.* vol. 23, pp. 085905, 2012.

[9] M.R. Moldover *et al*., "Acoustic gas thermometry," *Metrologia*, vol. 51, pp. R1–R19, 2014.

[10] J.B. Mehl *et al*., "Designing quasi-spherical resonators for acoustic thermometry," *Metrologia* vol. 41, pp. 295–304, 2004.

[11] S. Corbellini *et al*., "A Low-Cost Instrument for the Accurate Measurement of whispering-Gallery Resonances up to 19 GHz," *Proc. IEEE I2MTC2015*, May 2015.

[12] S. Corbellini, R.M. Gavioso, "A Low-Cost Instrument for the Accurate Measurement of Resonances in Microwave Cavities," *IEEE Tran. Instrum. Meas.* 2013, Vol. 62, Issue 5, pp. 1259–1266.

[13] S. Corbellini, "A Low-Cost Instrument for the Measurement of Microwave Resonances in Quasi-Spherical Cavities," *Proc. IEEE I2MTC2012*, May 2012.

[14] "IEEE Standard for Digitizing Waveform Recorders," *IEEE Instrum. Meas. Soc.*, IEEE Standard 1057–2007, 2007.

[15] M. Bertocco and C. Narduzzi, "Sine-fit versus discrete Fourier transform-based algorithms in SNR testing of waveform digitizers," *IEEE Trans. Instrum. Meas.*, vol. 46, no. 2, pp. 445Ű448, Apr. 1997.

[16] C-L. Cheng at al., "Highly accurate real-time GPS carrier phase-disciplined oscillator," *IEEE Tran. Instrum. Meas.*, vol. 54, no. 2, pp. 819–824, Apr. 2005.

[17] L. Pitre *et al*., "Acoustic thermometry: new results from 273K to 77K and progress towards 4K," *Metrologia*, vol. 43, pp. 142–162, 2006.

[18] L. Pitre *et al*., "Measurement of the Boltzmann constant kB using a quasi-spherical acoustic resonator," *Int. J. Theromphys.*, vol. 32, no. 9, pp. 1825–1866, 2011.

[19] J.B. Mehl, "Analysis of resonance standing-wave measurements," *J. Acoust. Soc. Am.*, 1978, Vol. 64, pp. 1523–1525.

Simone Corbellini was born in Italy in 1977. He received the M.S. degree in electronic engineering and the Ph.D. degree in metrology from Politecnico di Torino, Turin, Italy, in 2002 and 2006, respectively. He is currently an Assistant Professor with Politecnico di Torino. He is involved in the development of a measuring system for the accurate measurement of resonances in microwave resonators. His current research interests include digital signal processing, distributed measurement systems, and intelligent microcontroller-based instrumentation.

Chiara Ramella was born in Biella, Italy in 1985. She received the M.S degree in Electronic Engineering and the Ph.D. degree in Electronic Devices from Politecnico di Torino in 2009 and 2013, respectively. She is currently working as research assistant at University of Rome Tor Vergata in collaboration with Politecnico di Torino. Her research activities spread from low-noise analog electronic design to RF/microwave design and measurements.

Marco Pirola was born in Velezzo Lomellina, Italy, in 1963. He received the *Laurea* degree and Ph.D. in electronic engineering from Politecnico di Torino, Turin, Italy, in 1987 and 1992, respectively. In 1992 and 1994, he was a Visiting Researcher with the Hewlett Packard Microwave Technology Division, Santa Rosa, CA. Since 1992, he has been with the Department of Electronics and Communications, Politecnico di Torino, Turin, Italy, first as a Researcher and, since 2000, as an Associate Professor, where his research concerns the simulation, modeling, design, and measurements of microwave devices and systems.

Vito Fernicola is with the Thermodynamics Division of INRiM.

Andrea Cappella graduated in Physics at the Università degli studi of Trieste (Italy) in 2007. He joined the Temperature Group of the Metrology Institute of the Conservatoire National des Arts et Métiers (LNE-Cnam) in 2012 after completing his Ph.D. in Mechanical Engineering at Université de Bordeaux (France). His research activities after his Ph.D. were focused on the high temperature thermal characterization of thin film chalcogenide materials from the solid to the molten state. In particular, the development of a metrological facility for the thermal characterization of thin film materials. He is currently in charge of research activities in the design and realization of microwave based devices for temperature and humidity metrology. His main interests are mean and high temperature physics and electromagnetic behaviour of various systems.